A dissertation entitled

Harmonics and Instabilities in
Thyristor Based Switching Circuits

submitted to the Graduate School of the
University of Wisconsin-Madison
in partial fulfillment of the requirements for the
degree of Doctor of Philosophy

by

Sasan Ghombavani Jalali

Degree to be awarded: December 19 93 May 19___ August 19___

Approved by Dissertation Readers:

Major Professor

April 2, 1993
Date of Examination

Dean, Graduate School

HARMONICS AND INSTABILITIES IN THYRISTOR BASED SWITCHING CIRCUITS

Sasan Ghombavani Jalali
Under the supervision of Professor Robert H. Lasseter and
Assistant Professor Ian Dobson at the University of Wisconsin-Madison

This thesis investigates nonlinear dynamics, harmonic distortions and bifurcation instabilities in thyristor switching circuits. The analysis is directed towards the study of a Thyristor Controlled Reactor (TCR) which consists of a fixed reactor and two oppositely poled thyristors. The dependence of the thyristor switching times on the system states causes the circuit nonlinearities and is the focus of much of the thesis. New concepts for instability, dynamic response and damping for TCR circuits are introduced. These concepts are general and can be extended to other switching circuits. Useful TCR circuit examples such as the 230 kV Kayenta advanced series compensator and the 230 kV Rimouski static Var system are used to numerically verify these concepts. We have found new instabilities in both the Kayenta and the Rimouski systems in which switching times change suddenly, or bifurcate as a system parameter varies slowly. Switching time bifurcations are associated with large distortions of the TCR current or voltage waveforms leading to a new earlier TCR current zero, the disappearance of a current zero, or a

Acknowledgements

I would like to take this opportunity to thank my advisors, Professor Lasseter and Professor Dobson, for their patience and guidance throughout my doctoral studies.

My numerous meetings with Professor Lasseter helped me to define the problem and to keep in touch with the practical issues regarding it. Similarly, my numerous discussions with Professor Dobson provided me with the theoretical framework required in solving this problem.

The past three years of working together has given me the confidence to become an independent researcher, for which I am thankful.

Funding from EPRI under contracts RP 4000-29 and RP 8050-04 and from NSF PYI grant ECS-9157192 is gratefully acknowledged.

Table of Contents

List of Figures

Chapter 1

Introduction

Over the last couple of years there has been significant activity in the development of Flexible AC Transmission Systems (FACTS). Much of this work has been directed towards advanced series compensation (ASC) systems based on a thyristor controlled reactor connected in parallel with a fixed capacitor [8,9,17,18,28]. This results in a controllable series impedance element for use in transmission systems. As static switching circuits such as FACTS proliferate, there is an increasing need to analyze and understand these circuits and their interactions with power systems. However, because of the dependence of the thyristor turn on and off times on the system states, thyristor switching circuits are nonlinear and very awkward to analyze using standard mathematical techniques [17,25].

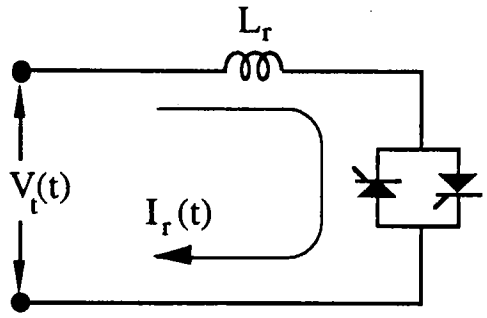

Figure 1.1. Basic single phase TCR

This thesis will use the Thyristor Controlled Reactor (TCR) circuit shown in the Figure 1.1 as an illustrative example for study. This circuit is a good choice for developing new techniques of analysis since the number of switching elements is small. Two useful TCR circuits are the

associated with the thyristor switching times, it is still one of the most common methods of computing eigenvalues [11,16,23,33]. We have found the average inductor model very useful in approximately predicting potential resonance points.

4) The dynamics of a switching circuits may be studied using state space averaging. It can be shown that averaging the state space equations is a good approximation for the pulse-width modulated convertors [34]. On the other hand, it can give incorrect results for the naturally commutated circuits such as the resonant link converters or the TCR circuits. Sanders in [39] extends this method to study the convertors which switch at lower frequencies by adding higher order correction terms to the classical formulation. However, it is not clear how this method can be used to study circuits with discontinuous modes of operation such as the thyristor controlled reactor.

5) The nonlinear dynamics of a TCR circuit were studied using the Poincare mapping from the dynamical systems theory [20,46]. In this approach, the system state is strobed at discrete times which are spaced by one period of the fundamental frequency, T and the system is studied by means of the Poincare map. The Poincare map advances the system state from one discrete time to the system state at the next discrete time. If the circuit has a steady state solution of period T, then the Poincare map has a fixed point. Except for marginal cases, the Poincare map can be differentiated and a formula for its Jacobian can be obtained. The Jacobian of the Poincare map evaluated at the fixed point can be used to

6) The harmonics of a power system which include a three phase thyristor bridge may be computed using the harmonic power flow method [51,52]. In this method, the AC current flowing into the converter terminal is solved in terms of the convertor AC voltage. One of the drawbacks is that the DC load is assumed to be a series combination of a resistor, inductor and a DC source. Another drawback is that the harmonic interactions of the converter and power system can not be studied when ambient even harmonics are present.

7) Peter Wood in [50] introduced the switching function method to compute the harmonics generated by converters which have fixed switching times. Bohmann and Lasseter extended this method to TCR circuits [7]. By expressing the TCR voltage and current as a Fourier series, a TCR harmonic admittance matrix is constructed. The admittance matrix is then incorporated into a power system providing a quick and general method to compute the power system harmonics. This method is explained in detail in chapter 3 and is used in chapter 5 to compute the harmonics of TCR circuits.

Classical analysis is often applicable, but can as demonstrated in this thesis and in [7,9] fail for certain circuit parameters and operating conditions. Under these conditions, both the voltage and the current waveforms become greatly distorted with large harmonic components. This phenomena is due to the circuit operating close to its resonance point and can be detected by the eigenvalues of the half wave Poincare map being -1.

coupling matrix which illustrates the coupling between the convertor voltage and current harmonics is developed. It is shown how this matrix can be incorporated into a power system and how the power system harmonics can be accurately calculated. In addition, an example system which exhibits large harmonic distortions and switching time bifurcation is also presented. In particular, it is shows that there may be two steady state solutions and/or no solutions over the regions for which the classical method predicts both the existence and the uniqueness of the solution.

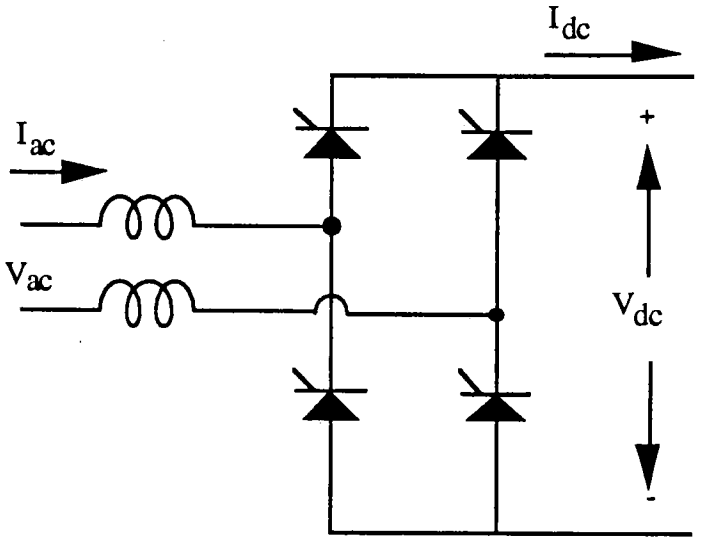

Figure 1.2 Single phase line commutated converter

Chapter 2

Thyristor Controlled Reactor (TCR)

Thyristor controlled reactors are typically composed of back to back thyristors used to vary the duty cycle of an inductor. In periodic steady state, the effect of the 60 Hz fundamental is to absorb varying amounts of reactive power from a power system network. Figure 2.1 shows a basic single phase Thyristor Controlled Reactor (TCR). It consists of a fixed reactor of inductance L (usually air core) and two oppositely poled thyristors which conduct on alternate half cycles of the supply frequency.

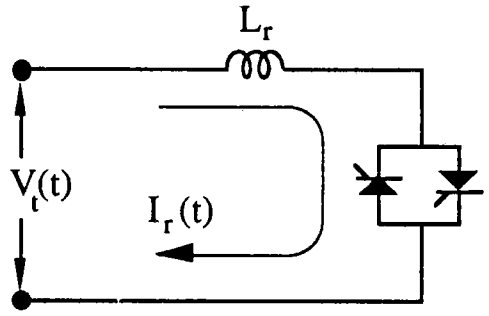

Figure 2.1. Basic single phase TCR

A thyristor conducts current only in the forward direction, can block voltage in both directions, turns on when a firing signal is provided and turns off after a current zero. The currently available thyristors can block a voltage range between 4000 to 6000 volts and can carry a current ranging from 2000 to 4000 amperes. In general, between 10 to 40 thyristor valves are connected in series to meet the required blocking voltage levels [21].

2.1 Two circuit examples using TCR

To illustrate some of the potential problems associated with the operation of TCR switching circuits and methods developed in this report, this section introduces two commonly used TCR circuits. These circuits are a single phase static VAR compensator and a single phase advanced series compensator.

The Static Var Compensator (SVC)

Figure 2.3 shows a SVC consisting of a thyristor controlled reactor (TCR) and a parallel capacitor. This system is connected to an infinite bus behind a power system impedance of an inductance L_s and a resistance R_s in series. The controlled reactor is modelled as a series combination of an inductor L_r and R_r.

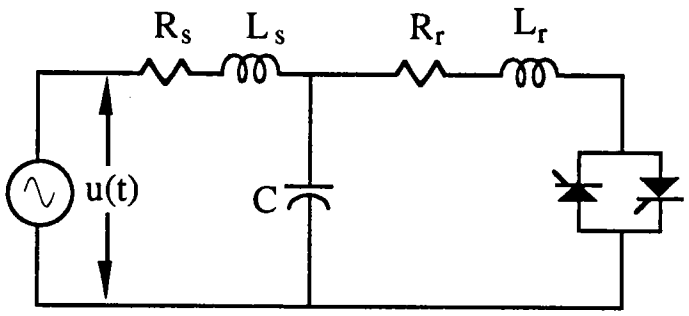

Figure 2.3. Single phase static VAR system

The above circuit can provide leading to lagging reactive power to the AC system. This characteristic behavior of the 60 Hz fundamental is approximately equivalent to an ideal system voltage source at the point of connection except that it has a limited range in which the voltage can be controlled.

been directed towards advanced series compensation (ASC) systems based on a thyristor controlled reactor connected in parallel with a fixed capacitor. This results in a controllable series impedance element for use in transmission systems.

Currently there are three such systems in various stages of commercialization. The Kanayna River system, West Virginia, is a joint R&D effort by American Electric Power Service Corporation and Asea Brown Boveri. This FACTS controller has been recently commissioned [32]. The system was planned to have 788 Mvar of series capacitance or 60% compensation. In the first phase of the project a prototype thyristor control module has been installed across one phase of 131 Mvar of compensation to create an ASC system. The remaining two phases will be installed following successful testing of this unit.

Western Area Power Administration is installing a 230 kV, 330 Mvar ASC system in northeastern Arizona at Kayenta Substation [8]. This system is supplied by Siemens AG. This scheme is comprised of 285 Mvar of conventional series capacitor banks with the remaining 45 Mvar of capacitance controlled by a parallel thyristor controlled reactor. Implementation of this FACTS scheme has progressed through the equipment development phases and currently is been installed at the site.

A third scheme is a major Electric Power Research Institute project with General Electric to develop a thyristor controlled series capacitor. A second phase of this project is to install such a system on a 500 kV transmission line in the Bonneville Power Administration region. This

2.2 Control methods and firing strategies

This section discusses the basic control issues and various firing schemes which are used to operate the TCR circuits.

Basic control scheme

Figure 2.5 shows a basic TCR control scheme with three function blocks. The first is the interface block which computes the root mean square of the TCR voltage. The second block is the regulator block. The input to this block is the difference between the reference quantities V_{ref} and the measured quantities V_{rms} and the output is a request value for either the thyristor conduction time σ or the firing delay α. The third block, the gate pulse generator, generates the firing pulses for the thyristors. The gate pulse generator usually uses one of the synchronization schemes described below so as to achieve the requested σ or α.

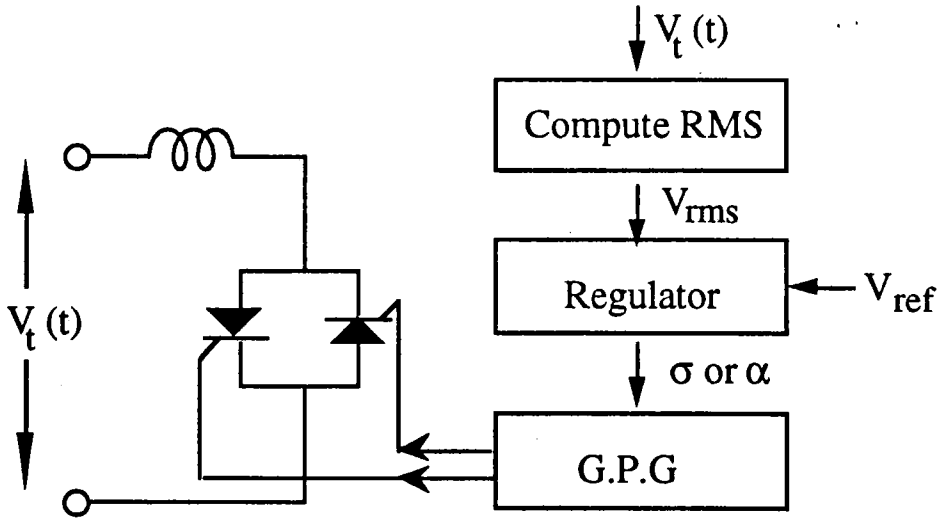

Figure 2.5. Control scheme for the TCR

parameter V_c. The phase of the equally spaced firing pulses has some arbitrary value with respect to the voltage across the TCR. In practice, this phase would drift relative to the TCR voltage. This is usually corrected by an external negative feedback loop.

An alternative to the phase locked loop scheme is shown in Figure 2.6 [4]. In this method, the firing pulses are sent whenever the integrator function V_{cf} intersects the controller output voltage V_c. At this point, the integrator V_{cf} is reset and the integration process starts again. The integrator function and the controller output voltage are chosen such that the firing pulses are spaced by 180 electrical degrees so that there are two firing pulses per cycle.

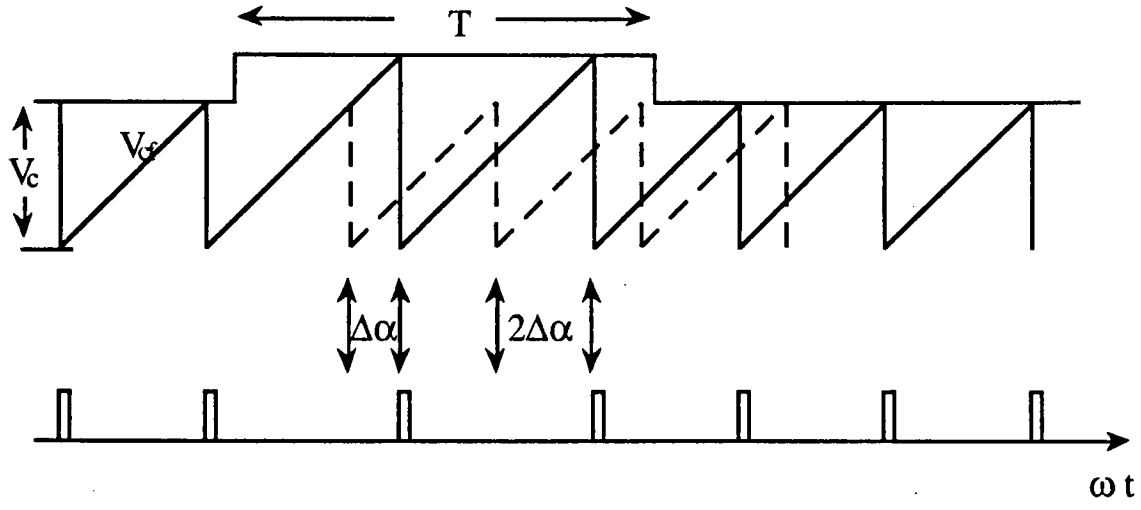

Figure 2.6. Firing pulses using the equidistant firing scheme

Figure 2.6 illustrates how the relative phase of the firing pulses can be changed by temporarily varying the control signal V_c. Let us assume that the firing pulses have initially a delay angle α with respect to the actual system. As long as the controller output voltage is fixed, α is also fixed

conduction and 1.0 when conduction. Integrating this signal results in an output which exhibits a slope change at the point where conduction stops. The output of the integrator is negatively biased by a constant value of 2π as shown in the Figure 2.7c. This signal is input to a zero plus detector which issues the firing pulses whenever the signal becomes positive. The resulting firing pulses are shown in the Figure 2.7d.

The main advantage of this scheme is that there is no need for accurate measurement of either voltage or current.

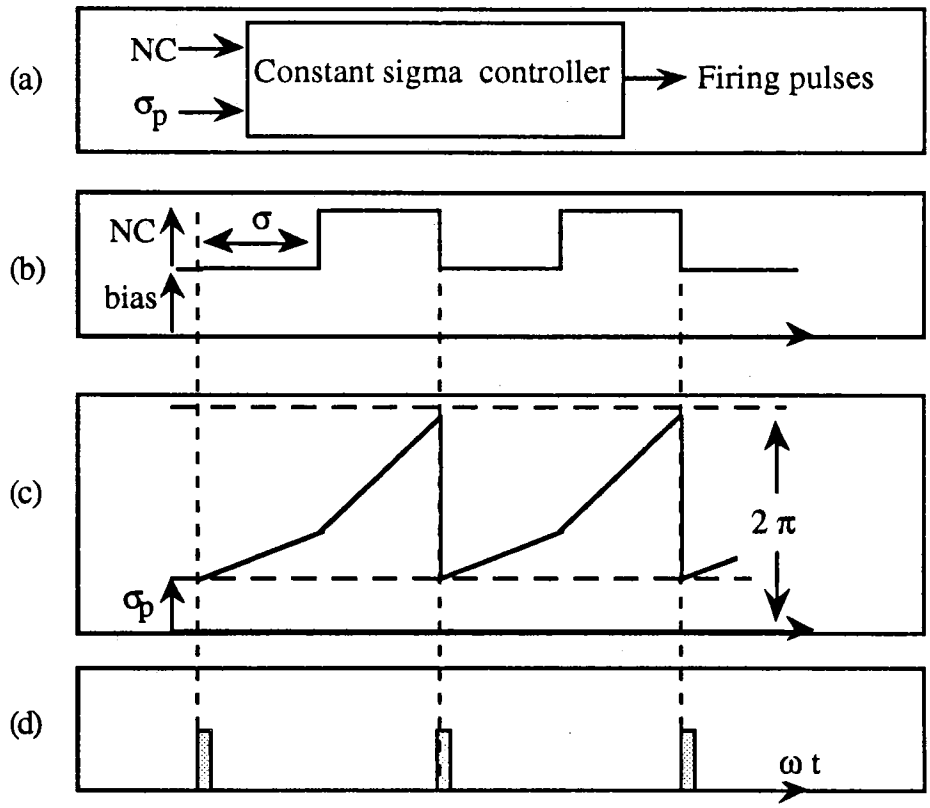

Figure 2.7. The constant sigma controller

Chapter 3

Tools to Study the Thyristor Controlled Reactor

A thyristor controlled reactor (TCR) is a thyristor based compensator which is capable of absorbing reactive power from a power system network. In chapter 2, issues associated with the control and operation and firing strategies for two useful TCR circuits were studied. These two TCR circuits are, the Static Var Compensator (SVC) and the Advanced Series Compensator (ASC) shown in Figures 1 and 2.

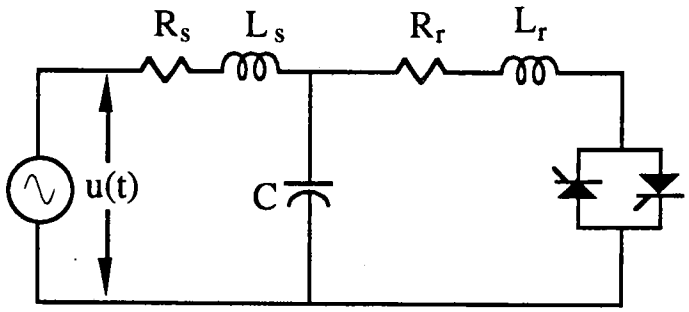

Figure 3.1. Single phase static VAR compensator

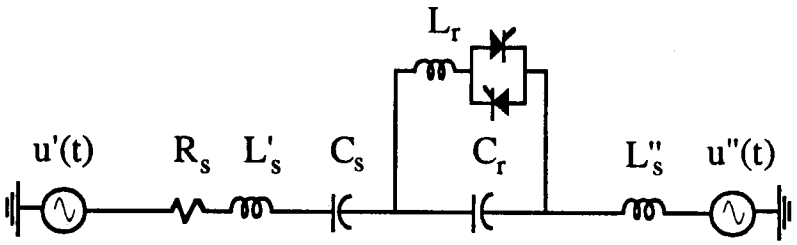

Figure 3.2. Advanced series compensator

In section 3.1, the classical method of computing the system harmonics is explained. Section 3.2 introduces a simple average inductor model useful in approximately predicting potential problems with the operation

shown by the gray line in the Figure 3.3. In the classical analysis, the two variables σ and α are commonly used in explaining the TCR operation. σ denotes the conduction time of a thyristor while α is the firing point relative to the voltage across the thyristor. These two variables are related by $2\alpha + \sigma = 2\pi$. Therefore, if the thyristors are fired at the point where the TCR voltage is at a peak, ($\alpha = \pi/2$), full conduction results ($\sigma = \pi$). If the firing is delayed from the peak voltage, the current becomes discontinuous with a reduced fundamental component of reactive current. This partial conduction is obtained with firing angles between 90 and 180 electrical degrees.

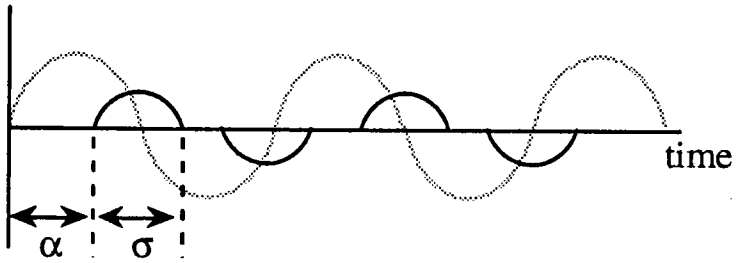

Figure 3.3. Classical operation of a TCR

The classical analysis provides a two step process by which the power system harmonics can be computed as described below.

Harmonics in a static VAR compensator

First the TCR is modelled as an equivalent harmonic current source:

$$I_{tcr}(\omega t, \sigma) = \sum_{n=1}^{n=\infty} I_n(\sigma) e^{jn\omega t} \qquad (3.1)$$

$$V_{tcr}(\omega t,\sigma)=\sum_{n=1}^{n=\infty}V_n(\sigma)e^{jn\omega t} \qquad (3.2)$$

where $V_n(\sigma)$ is the nth harmonic of $V_{tcr}(\omega t,\sigma)$. To compute $V_{tcr}(\omega t,\sigma)$, the AC system as seen from the TCR terminals is replaced by a Thevenin current source $I_{th}(\omega t)$ in parallel with a Thevenin capacitance C_{th} as shown in the Figure 3.7 [8,9].

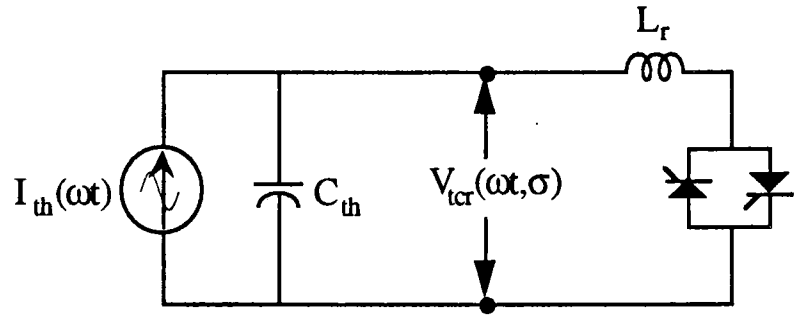

Figure 3.6. Classical method of computing $V_{tcr}(\omega t,\sigma)$ in an ASC

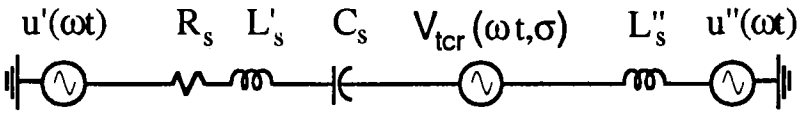

Figure 3.7. Classical method of computing harmonics in an ASC

Power system harmonics are then calculated by replacing the TCR and C_r with $V_{tcr}(\omega t,\sigma)$ as shown in the Figure 3.5. This method ignores the important harmonic interaction between the TCR and the power system.

3.2 Average inductor model

The average inductor model is a simple and useful method in approximately predicting potential problems with the operation of a TCR. In this model, the TCR is represented as a variable inductance

The harmonic resonant frequency of the system can be computed from the above equivalent model as:

$$f_{res} = \frac{1}{2\pi}\sqrt{\frac{1}{C L_s} + \frac{1}{C L_{eq}(\sigma)}} \qquad (3.4)$$

Equation (3.4) implies that the static var system harmonic resonance frequency depends on the conduction time, σ, of the TCR and the inductive and capacitive components. For example, typical values of system inductance, fixed capacitor and variable inductance can have resonance at the 5th harmonic. In this case, this model predicts that the system experiences large harmonic voltages and currents.

Advanced series compensator

Figure 3.9 shows the application of the average inductor model to the advanced series compensator example with all the circuit resistances are ignored.

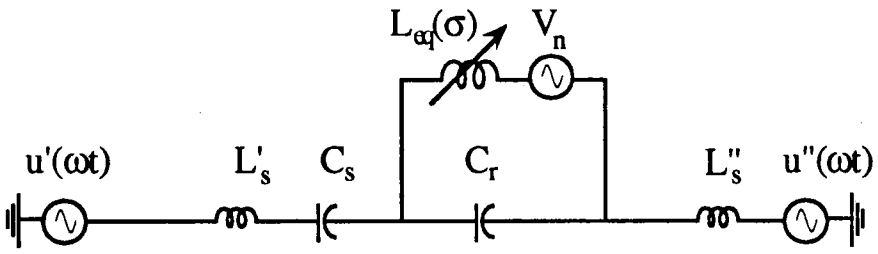

Figure 3.9. Modelling the ASC with an average inductor model

The resonant frequency of this system can be computed from the above equivalent model and is given by:

$$f_{res} = \frac{1}{2\pi}\sqrt{A + \sqrt{A^2 - \frac{1}{C_r C_s L_s L_{eq}(\sigma)}}} \qquad (3.5)$$

The switching function, H(ωt), shown in Figure 3.11 has a value of one whenever a thyristor is on and zero when the thyristors are off. Since a thyristor turns off when its current goes through zero, the conduction time, σ depends on the turn on time ϕ, the terminal voltage $V_t(\omega t)$ and the TCR reactance L_r. Therefore the switching function is dependent on the terminal voltage through the turn on/off time of the thyristors.

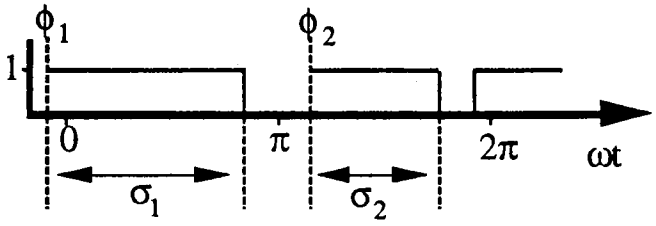

Figure 3.11. The switching function, H(ωt)

The voltage across the TCR inductance $V_r(\omega t)$ is the product of the switching function H(ωt) by the terminal voltage $V_t(\omega t)$. Assuming periodicity, the Fourier components of H(ωt), $V_t(\omega t)$ and $V_r(\omega t)$ are related by the matrix equation (for details see the appendix A):

$$\begin{bmatrix} \cdot \\ \cdot \\ v_{r-3} \\ v_{r-2} \\ v_{r-1} \\ \cdot \\ \cdot \end{bmatrix} = \begin{bmatrix} \cdot & \cdot & \cdot & \cdot & \cdot & \cdot & \cdot \\ \cdot & \cdot & \cdot & \cdot & \cdot & \cdot & \cdot \\ \cdot & \cdot & h_0 & h_{-1} & h_{-2} & \cdot & \cdot \\ \cdot & \cdot & h_1 & h_0 & h_{-1} & \cdot & \cdot \\ \cdot & \cdot & h_2 & h_1 & h_0 & \cdot & \cdot \\ \cdot & \cdot & \cdot & \cdot & \cdot & \cdot & \cdot \\ \cdot & \cdot & \cdot & \cdot & \cdot & \cdot & \cdot \end{bmatrix} \begin{bmatrix} \cdot \\ \cdot \\ v_{t-3} \\ v_{t-2} \\ v_{t-1} \\ \cdot \\ \cdot \end{bmatrix} \qquad (3.6)$$

where h_n is a function of $\sigma_1, \phi_1, \sigma_2$ and ϕ_2. The above matrix equation illustrates the coupling between the harmonics which is an important

bus connecting the TCR to the external system as shown in Figure 3.12. Without the TCR connected, the resulting linear system has a harmonic Z_{th} matrix.

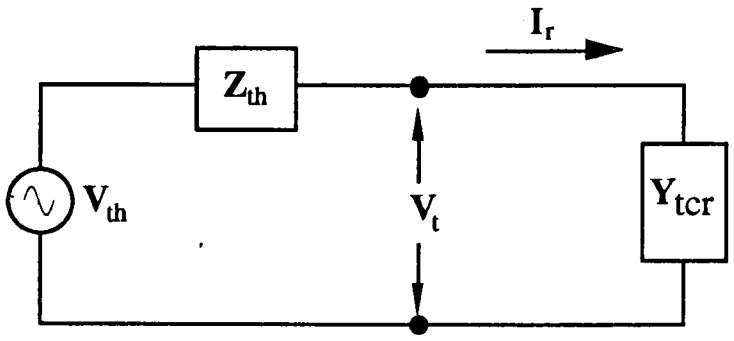

Figure 3.12. The reduced equivalent system

The equivalent system impedance is the diagonal element of the $\mathbf{Z}_{th}$ matrix corresponding to the TCR bus. In the equivalent system shown the voltage across the terminals is:

$$\mathbf{V}_t = \mathbf{V}_{th} - \mathbf{Z}_{th}\,\mathbf{I}_r \qquad (3.10)$$

Using $\mathbf{I}_r$ given in equation (3.9) allows an expression for $\mathbf{V}_t$ to be written. ($\mathbf{I}$ is the identity matrix)

$$\mathbf{V}_{th} = [\ \mathbf{I} + \mathbf{Z}_{th}\,\mathbf{Y}_{tcr}(\sigma_1,\phi_1,\sigma_1,\phi_1)\ ]\,\mathbf{V}_t \qquad (3.11)$$

The zero thyristor current at the switching times $(\phi_1+\sigma_1)$ and $(\phi_2+\sigma_2)$ define two relationships between the times σ_1, ϕ_1, σ_2 and ϕ_2 and the terminal voltage harmonics as derived in the appendix A. These are:

$$0 = v_{t0}\sigma_i + \sum_{m=-\infty}^{\infty} \frac{v_{tm}}{jm}\left[e^{-jm(\phi_i+\sigma_i)} - e^{-jm\phi_i}\right] \qquad \text{for } i=1,2 \qquad (3.12)$$

Rewriting the above equations yields the following two relationships between the thyristor switching times.

$$\sigma_{req} = \frac{\sigma_1 + \sigma_2}{2} \tag{3.16}$$

$$\phi_2 - \phi_1 = \pi + \frac{\sigma_1 - \sigma_{req}}{2} \tag{3.17}$$

The control parameter σ_{req} takes a value from 0 to π where σ_{req} is a given control point. Equations (3.11) and (3.12) together with (3.16) and (3.17) give us a complete set of equations to solve for the periodic solutions of the system under the constant sigma controller. Note that if the periodic solution is half wave symmetric we have $\sigma_1=\sigma_2=\sigma_{req}$ otherwise, σ_{req} represents the average of the two conduction lengths. The suggested solution algorithm is to use the Newton's method as was done earlier for the equidistant firing controller. For initial guess, one may solve (3.11) for $\mathbf{V}_t$ by choosing $\sigma_1=\sigma_2=\sigma_{req}$, $\phi_2=\phi_1+\pi$ and

$$\phi_1 = \pi - \frac{\sigma_{req}}{2} \tag{3.18}$$

Computation with the infinite harmonic system vectors and matrices are made by assuming the higher harmonic terms can be neglected. From the details in the appendix, it is seen that the elements in the switching matrix **H**, which defines $\mathbf{Y}_{tcr}$ fall off as 1/n. The harmonics in power systems will generally do the same. This allows the higher harmonics to be ignored. The vectors and matrices can therefore be truncated at a harmonic number above the harmonics of interest.

A thyristor conducts current only in the forward direction, can block voltage in both directions, turns on when a firing signal is provided and turns off after a current zero. The thyristors are assumed ideal so that the nonlinearity of the circuit only arises from the dependence of the switch on and off times of the thyristors on the system state.

During the thyristor conduction time, the system state vector x(t) specifies the TCR current, voltage, the line current and the fixed series capacitor voltage:

$$x(t) = \begin{bmatrix} I_r(t) \\ V_r(t) \\ I_s(t) \\ V_s(t) \end{bmatrix} \tag{3.19}$$

The system input u(t)=u'(t)-u"(t) is the net source voltage which is assumed to be periodic with period T and the system dynamics are described by the following set of linear differential equations:

$$\dot{x}(t) = Ax(t) + Bu(t) \tag{3.20}$$

where

$$A = \begin{bmatrix} 0 & 1/L_r & 0 & 0 \\ -1/C_r & 0 & 1/C_r & 0 \\ 0 & -1/L_s & -R_s/L_s & -1/L_s \\ 0 & 0 & 1/C_s & 0 \end{bmatrix} \text{ and } B = \begin{bmatrix} 0 \\ 0 \\ 1/L_s \\ 0 \end{bmatrix} \tag{3.21}$$

During the off time of each thyristor, the circuit state is constrained to lie in the plane $I_r=0$ of zero thyristor current. In this mode, the system

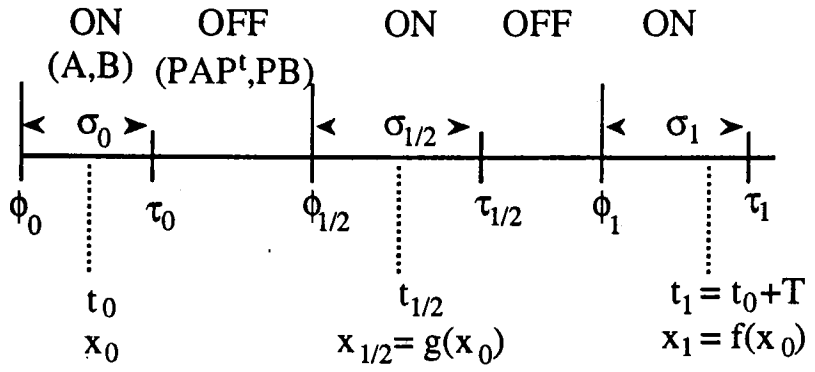

Figure 3.14. ASC system dynamics from time ϕ_0 to τ_1.

The thyristor turn on times at $\phi_{1/2}$ and ϕ_1 depend on the firing scheme and the closed loop control. We study the open loop system when operated with one of the four common firing schemes. These are equidistant firing, constant sigma controller and synchronization on the ASC voltage or the ASC line current.

(a) In equidistant firing the thyristor turn on pulses are supplied periodically and the system is controlled by varying the phase of the firing pulses, ϕ. Since the relationship between ϕ and the TCR firing angle α depends on the line impedance, a negative feed back loop modifying ϕ is usually used to ensure a requested α. In this section, we restrict our analysis to an equidistant firing with no feed back control i.e., the thyristor turn on times are computed using a requested phase delay ϕ_{req} as follows:

$$\phi_{1/2} = \frac{T}{2} + \phi_{req} \tag{3.25}$$

$$\phi_1 = T + \phi_{req} \tag{3.26}$$

$$\phi_1 = \alpha_{reqc} + \tau_{c1/2} \tag{3.32}$$

The state at the switch on time ϕ_0 is denoted either by the vector $y(\phi_0)$ or by the vector $x(\phi_0)$. These representations of the state at the switch on time are related by

$$x(\phi_0)=P^t\, y(\phi_0) \tag{3.33}$$

Equation (3.33) expresses the fact that the state in x coordinates at a switch on is computed from the y coordinates by adding a first component which has value zero. The state at the switch off time τ_0 is similarly denoted either by $x(\tau_0)$ or $y(\tau_0)$ and these are related by

$$y(\tau_0)=P\, x(\tau_0) \tag{3.34}$$

The matrix P in equation (3.34) may be thought of as projecting the vector x onto the hyperplane of zero thyristor current. Given a time interval $[s_1,s_2]$, it is convenient to write $f(.,s_1,s_2)$ for the map which advances the state at s_1 to the state at s_2. For example, a Poincare map which advances the state by one period T starting at time t_0 may be written $f(x,t_0,t_0+T)$. For convenience, we adopt the notation that when the thyristor is on during all of the time interval $[s_1,s_2]$, we write $f(x,s_1,s_2)$ as $f_{on}(x,s_1,s_2)$. Similarly, if the thyristor is off during $[s_1,s_2]$, we write $f(y,s_1,s_2)$ as $f_{off}(y,s_1,s_2)$. f_{on} or f_{off} can be computed by integrating the linear system (3.20) or (3.23) over the corresponding time intervals.

$$f(x_0,t_0,t_{1/2})=f_{on}(P^t\, f_{off}(P\, f_{on}(x_0,t_0,\tau_0),\tau_0,\phi_{1/2}),\phi_{1/2},t_{1/2}) \qquad (3.39)$$

The Poincare map may now be written by composing two successive half cycle maps and then neglecting the gory details of the time arguments:

$$f(x_0,t_0,t_0+T) = f_{on}\, P^t\, f_{off}\, P\, f_{on}\, P^t\, f_{off}\, P\, f_{on}\, x(t_0) \qquad (3.40)$$

We assume that gradient of the thyristor current as it turns off is negative so that the Poincare map is smooth and differentiable.

Important Simplification

Let $[s_1, s_2]$ be a fixed time interval including a thyristor turn off at time τ and no other switchings. For convenience, let x_1 express the state at time s_1. Define $H(x_1,\tau)$ as:

$$H(x_1,\tau) = f_{off}(P\, f_{on}(x_1,s_1,\tau),\tau,s_2) = \qquad (3.41)$$

$$= e^{PAP^t(s_2-\tau)}Pe^{A(\tau-s_1)}[x_1 + \int_{s_1}^{\tau} e^{A(s_1-\alpha)}Bu(\alpha)d\alpha] + \int_{\tau}^{s_2} e^{PAP^t(s_2-\alpha)}PBu(\alpha)d\alpha$$

Note that H expresses $y(s_2)$ as a function of x_1 and the switch off time τ. τ is a function of x_1 which is determined by the constraint of zero thyristor current at time τ. The map $f(x_1,s_1,s_2)$ which advances the state x_1 to the state $y(s_2)$ is equal to:

$$f(x_1,s_1,s_2) = H(x_1,\tau(x_1)) \qquad (3.42)$$

The chain rule gives:

Despite the simplification, it is sometimes necessary to compute $D\tau$. The equation which determines the thyristor turn off time τ is the first positive root of:

$$0 = cx(\tau) = ce^{A(\tau - s_1)}[x_1 + \int_{s_1}^{\tau} e^{A(s_1 - \alpha)}Bu(\alpha)d\alpha] \tag{3.47}$$

where c=(1,0,0,0). Differentiation with respect to s_1 and solving for $D\tau$ yields:

$$D\tau = \frac{-ce^{A(\tau - s_1)}}{c(Ax(\tau) + Bu(\tau))} = \frac{-ce^{A(\tau - s_1)}}{c\dot{x}(\tau -)} \tag{3.48}$$

Note that $c\dot{x}(\tau -)$ (the limit of $c\dot{x}(t)$ as t approaches τ from below) is the gradient of the thyristor current as it turns off at τ.

Jacobian and stability

When the ASC is in steady state with a periodic trajectory of period T, the Poincare map has a corresponding fixed point. That is,

$$f(x(t_0),t_0,t_0+T)=x(t_0) \tag{3.49}$$

The stability of a periodic orbit is the same as the stability of the corresponding fixed point of the Poincare map [6,7]. That is, the stability of the periodic orbit can be computed from the Jacobian of the Poincare map evaluated at the fixed point. In particular, the periodic orbit is exponentially stable if the eigenvalues of the Jacobian lie inside the unit circle. Since the thyristor turn off time and the Poincare map

$$\frac{\partial H_0}{\partial \phi_{1/2}} = -e^{(t_{1/2}-\phi_{1/2})} c^t c\dot{x}(\phi_{1/2}+) \tag{3.55}$$

where $c\dot{x}(\phi_{1/2}+)$ is the gradient of the TCR current as it turns on at $\phi_{1/2}$. In (3.53), the row vector $D\phi_{1/2}$ is the gradient of the turn on time $\phi_{1/2}$ with respect to x_0. This term depends on the firing scheme as follows:

a) In an equidistant firing, $\phi_{1/2}=(T/2)+\phi_{req}$ as given in (3.25). Hence $D\phi_{1/2}=0$. This is the simplest firing scheme i.e. the turn on time does not depend on the system state.

b) In the constant sigma controller, $\phi_{1/2}=(\phi_0+ \tau_0+ 2\pi- \sigma_{req})/2$ as given in (3.27). ϕ_0 and τ_0 are the previous turn on and turn off times. Both are dependent on x_0. Differentiation yields:

$$D\phi_{1/2} = \frac{D\phi_0+D\tau_0}{2} \tag{3.56}$$

where $D\phi_0$ and $D\tau_0$ represent the gradient of the turn on time ϕ_0 and turn off time τ_0 with respect to x_0. By analogy with (3.48), $D\tau_0$ and $D\phi_0$ are equal to:

$$D\tau_0 = \frac{-ce^{A(\tau_0-t_0)}}{c\dot{x}(\tau_0-)} \tag{3.57}$$

$$D\phi_0 = \frac{-ce^{A(\phi_0-t_0)}}{c\dot{x}(\phi_0+)} \tag{3.58}$$

where c=(1,0,0,0), and the terms in the denominator denote the gradients of the TCR current as it turns on at ϕ_0 and turns off at τ_0.

Note that $H_{1/2}$ expresses $x(t_1)$ as a function of $x_{1/2}$, the turn off time $\tau_{1/2}$ and the turn on time ϕ_1. $\tau_{1/2}$ is a function of $x_{1/2}$ which is determined by the constraint of zero thyristor current at time $\tau_{1/2}$. The turn on time ϕ_1 may or may not depend on $x_{1/2}$ depending on the firing strategy. Then the second half cycle map $f(x_{1/2}, t_{1/2}, t_1)$ is equal to:

$$f(x_{1/2},t_{1/2},t_1) = H_{1/2}(x_{1/2},\tau_{1/2}(x_{1/2}),\phi_1(x_{1/2})) \tag{3.62}$$

Using the chain rule and the simplification, the $Df(x_{1/2}, t_{1/2}, t_1)$ is equal to:

$$Df(x_{1/2},t_{1/2},t_1) = \frac{\partial H_{1/2}}{\partial x_{1/2}} + \frac{\partial H_{1/2}}{\partial \phi_1} D\phi_1 \tag{3.63}$$

where each term in the right hand side can directly be written from its corresponding term as defined in the equations (3.53) to (3.60) by replacing all the subscripts "1/2" by "1" and the subscripts "0" by "1/2". Next, using the chain rule, the Jacobian of the Poincare map is given by:

$$Df(x_0,t_0,t_1) = Df(x_{1/2},t_{1/2},t_1)\ Df(x_0,t_0,t_{1/2}) \tag{3.64}$$

where $Df(x_{1/2},t_{1/2},t_1)$ and $Df(x_0,t_0,t_{1/2})$ are given by (3.53) and (3.63).

Simplifications for symmetric periodic orbits

It is convenient to take advantage of symmetry when the periodic orbits are half wave symmetric. Half wave symmetry of a periodic orbit means that the system states are equal in magnitude and opposite in sign to the

quantitative method which provides little understanding of the important interactions.

Lasseter has shown how the ElectroMagnetic Transient Program (EMTP) [10] can be used to simulate TCR switching circuits using different firing strategies. In particular, it is shown how the constant sigma controller firing strategy can be modelled through the EMTP. All of the time domain simulations in this report are done using the EMTP as the simulation program.

3.6 Summary

Both conventional and novel tools for studying TCR circuits were discussed. Frequency plane analysis suffers from the simplification required to achieve a solution. Section 3.3 describes how Fourier techniques can be used to construct a TCR harmonic admittance matrix. The admittance matrix can then be incorporated into a power system providing a quick method to calculate system harmonics. Section 3.4 studies the nonlinear circuit dynamics of an advanced series compensator using the Poincare mapping from dynamical systems theory. It is shown how the thyristor turn off time may be regarded as a fixed turn off time when deriving the system Jacobian. This fact results in a simple and useful formula for the Jacobian matrix of the Poincare map when the TCR is operating with an equidistant firing. It is also shown how correction terms may be added to the simple formula to compute the Jacobian matrix when the TCR is operating with other firing schemes.

Chapter 4

Bifurcations, Harmonic Distortions and Resonance

The classical analysis is often applicable, but can fail for certain circuit parameters and operating conditions. Under these conditions, the TCR current and voltage waveforms can become highly distorted. These large harmonic distortions are associated with the natural frequencies of the circuit, from when the reactor is fully on to when it is fully off, spanning an odd harmonic number. Section 4.1, discusses the large harmonic distortions to the circuit operating close to its resonance point. It is shown how this resonance point may be predicted through the computation of the eigenvalues. The large harmonic distortions can lead to instabilities associated with either a new earlier TCR current zero, the disappearance of the TCR current zero or a thyristor misfire (section 4.2). These instabilities, called switching time bifurcations, are very different from conventional bifurcations in that they are not detected by the eigenvalues the Jacobian matrix crossing the unit circle. However, different firing schemes can introduce conventional bifurcations just before a switching time bifurcation (section 4.4).

4.1 Resonance and harmonic distortions

Lasseter and Bohmann showed that a single phase SVC circuit can exhibit behavior much like resonance in a linear circuit for certain parameter values [7]. In particular, resonance is expected when the resonant frequency of the circuit from when the TCR is fully on to when it is fully

3.4). g(.) is a bounded function with terms involving the integration of the input over the period. Rewriting (4.3) as:

$$-(I+DH)^{-1}\, g(\sigma,\phi_0) = y_0 \qquad (4.4)$$

shows that y_0 becomes unbounded as an eigenvalue of DH approaches -1. Chapter 5 shows four TCR circuit examples in which DH has eigenvalue approaching -1 for different values of σ.

4.2 Switching time Bifurcations

When the harmonic components of the TCR current and voltage become very large, the current and voltage waveforms become highly distorted. These distortions can lead to instabilities as switching times suddenly change or bifurcate as follows:

Instability when a new TCR current zero appears

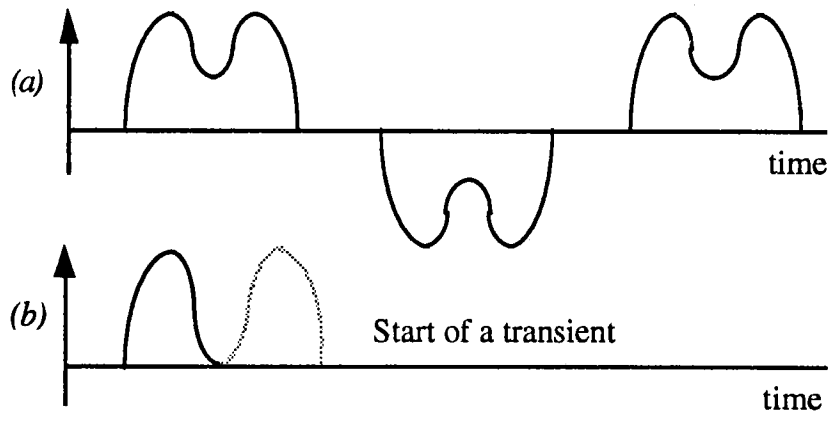

Figure 4.1. A new earlier TCR current zero appears
(a) $\phi < \phi^*$, (b) $\phi = \phi^*$

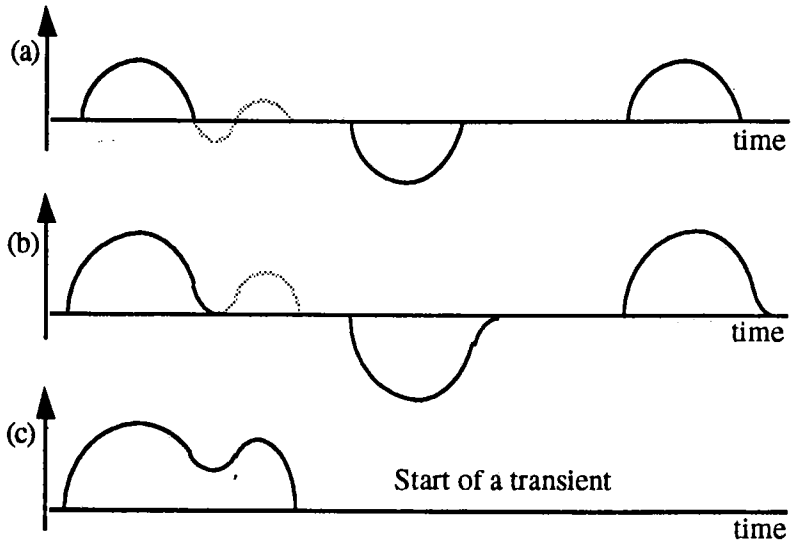

Figure 4.2. Disappearance of two TCR current zeros
(a) $\phi < \phi^*$ *, (b)* $\phi = \phi^*$ *,(c)* $\phi > \phi^*$

Instability due to a thyristor misfire

Figure 4.3 explains the onset of instability due to a thyristor misfire [26,38]. The TCR current is denoted with the solid line in the Figure 4.3a and starts conducting, as expected, when a firing pulse is applied. The gray lines in Figure 4.3 are used to show the thyristor current that would have obtained if we would have integrated the system backwards in time with the thyristor on and with the initial TCR current of zero at the firing time. As the firing pulses are moved towards the zero crossings of the TCR voltage, the TCR voltage blocked by the thyristors at the firing time decreases. Assuming thyristors are ideal, the critical phase ϕ^* occurs when the turn on firing pulse is sent at the zero crossings of the TCR voltage as shown in the Figure 4.3b. As the phase ϕ slightly increases from ϕ^*, one of the thyristors misfires as the voltage across it is negative when the firing pulse arrives. In practice, the